J MATER SCI 41 (2006) 3071–3082

Carbonation process of alkali-activated slag mortars

F. PUERTAS*, M. PALACIOS, T. VÁZQUEZ
Eduardo Torroja Institute (C.S.I.C), Serrano Galvache n° 4, 28033 Madrid, Spain
E-mail: puertasf@ietcc.csic.es

Published online: 18 October 2005

This study analyzes the behaviour of waterglass- or NaOH-activated slag mortars after carbonation. The effect of a superplasticizer based on vinyl copolymer and shrinkage reducing polypropylenglycol derivative admixtures on that process was also examined. The same tests were run on cement mortars for reference purposes.
The mortars were carbonated in a chamber ensuring CO_2 saturation for four and eight months, after which ages the samples were tested for mechanical strength; mercury porosimetry and mineralogical (XRD, FTIR) and microstructural characterization (SEM/EDX) were also conducted. The results obtained indicate that alkali-activated slag mortars were more intensely and deeply carbonated than Portland cement mortars. Carbonation took place directly on the gel, causing decalcification. When waterglass was the alkaline activator used, carbonation caused a loss of cohesion in the matrix and an important increase in porosity and decrease in mechanical strength. When a NaOH solution was used as the alkali activator, carbonation enhanced mortar compaction and increased mechanical strength. Finally, in waterglass-activated slag mortars, the inclusion of organic admixtures had no effect either on their behaviour after carbonation or the nature of the reaction products. © *2006 Springer Science + Business Media, Inc.*

1. Introduction

The basic principles and initial approach to using alkali-activated blast-furnace slag as a binder for the construction industry were developed in 1957 by V.D. Glukhosvskii *et al*. [1, 2]. These studies laid the groundwork for new binders whose manufacture is much less energy-intensive and more environment-friendly than the production of ordinary Portland cement (OPC). Indeed, the manufacturing process benefits not only from low energy requirements, but uses industrial waste as a raw material and drastically reduces the emission of greenhouse gases (CO_2, SO_2, NO_X). It was not until the 90's, however, that researchers in other countries began to take an interest in such alkali-activated slag (AAS) cement and concrete [3–8].

Today the focus is no longer on obtaining new binders, but on developing materials with sustainably high mechanical strength. AAS cement can reach compression strengths of up to 30–40 MPa at the age of 24 h, and these values rise with time. Other authors have also proven the chemical stability of these cements and concretes when attacked by sulphates [9], seawater [10], chlorides [11], acid media [12, 13], frost-thaw cycles [14, 15], high temperatures [16, 17], and so on. Such excellent performance is due to the nature of the hydration products [18–20], and low concrete porosity and permeability [5].

Another important consideration in connection with concrete durability is carbonation, which can cause the depassivation and subsequent corrosion of reinforcing steel. The carbonation of Portland cement concrete is a widely studied and well understood process [21, 22]. Far fewer studies have been conducted on AAS cement and concrete, however. The earliest papers were published by Byfors *et al*. [23], who concluded that F-concrete (blast furnace slag activated by a combination of alkali metal compounds and which contains lignosulphonates) had a higher carbonation rate than Portland cement concrete with the same compression strength; they added, however, that with concrete covers of over 30 mm, corrosion would not take place for the first sixty years of a structure's service life. Pu *et al*. [24] showed that there was a relationship between AAS concrete strength and its carbonation rate: they established that concrete with strengths of under 30 MPa had a high carbonation rate, those with a strength of from 30 to 50 MPa had a medium rate and when the

*Author to whom all correspondence should be addressed.
0022-2461 © *2006 Springer Science + Business Media, Inc.*
DOI: 10.1007/s10853-005-1821-2

strength was over 50 MPa, the rate and degree of carbonation were comparable to the values found for concrete made with Portland cement.

Deja [25] and Bakharev *et al*. [26] deduced that AAS concrete carbonated more rapidly than the respective Portland concrete. Yet their descriptions of the effects of such carbonation differed substantially. While Deja concluded an increase in the mechanical strength of carbonated mortars, strength was observed to decline after carbonation in the concrete studied by Bakharev *et al*. The latter authors sustained that the mechanism involved in carbonation to be the action of CO_2 on the calcium silicate hydrated (CSH) gel.

Moreover, the nature of the alkali activator also appears to affect the carbonation rate and intensity in this type of mortars. Some authors [25] believe that carbonation is shallower when a waterglass solution ($Na_2O{\cdot}nSiO_2{\cdot}mH_2O$ + NaOH) is used as the activator, although this is not sufficiently clear.

Unlike the foregoing researchers, Xu Bin and Pu Xincheng [15] showed that the carbonation rate is lower in AAS than in Portland cement pastes. These authors interpreted their results on the basis of two different developments: they found, firstly, that low alkalinity hydrates (such as a CSH gel in an AAS paste) resisted carbonation better and vice-versa; and secondly that the carbonation reaction in the concrete depended on the water content and concentration of atmospheric CO_2. They concluded that given its low permeability, AAS concrete was less susceptible to penetration by water and CO_2 than Portland cement concrete.

In light of such obvious discrepancies, the aim of the present research is to study the carbonation of different types of AAS mortars and pastes prepared with a number of combinations of alkali activators and organic admixtures. This study explains how the process progresses and its mechanical and microstructural consequences.

2. Experimental

2.1. Materials and mortar preparation

Spanish granulated blast-furnace slag from a factory located at Avilés, Asturias, and CEM I 42.5 Portland cement were used in this study. The chemical composition of the two materials is shown in Table I and their particle size distribution is described in Table II.

The composition of the different mortars prepared is shown in Table III. The aggregate/binder ratio of these AAS and cement mortars was 2:1. Spanish and European standard UNE-EN 196-1 sand with a SiO_2 (quartz) content of over 98% was used. One of the mortars was prepared using only Portland cement and the others were AAS mortars. Of these AAS mortars, three were activated with waterglass solution, with a Na_2O/SiO_2 ratio of 0.85, and one was activated with NaOH solution. Of the three waterglass-activated slag mortars, the first contained no additives, while the others contained a vinyl co-polymer (V) or a shrinkage-reducing admixtures (SRA). Table IV gives some of the properties of these admixtures. The admixture was blended into the mortar with the activator solution in dosages of 1% by mass of the slag. The liquid/solid (l/s) ratio used was determined by the slump test described in Spanish standard UNE-80-116-86.

TABLE I Chemical composition of blast-furnace slag and cement

	CEMENT	SLAG (99% vitreous phase)
P.F*	0,78	2,02
SiO_2	19.97	34,95
R.I.**	0,29	0,11
Al_2O_3	5,17	13,11
Fe_2O_3	3,85	0,69
CaO	64,41	41,37
MgO	1,30	7,12
SO_3	2,64	0,04
S^{2-}	–	1,92
Na_2O	0,39	0,27
K_2O	0,78	0,23
CaO free	0,22	–

*P.F. Loss on ignition; **R.I. Insoluble residue.

TABLE II Slag and cement particle size distribution

	Particle diameter (μm)	
% volume	CEMENT	SLAG
10.0	2.16	0.94
25.0	9.12	4.28
50.0	20.49	13.13
75.0	34.31	25.17
90.0	47.45	38.44
Specific surface (Blaine)	360 m^2/kg	325 m^2/kg

TABLE III Mortars prepared

Mortar	Composition	l/s ratio
A	Cement	0.42
B	Slag + Waterglass	0.58
C	Slag + Waterglass + 1% SRA	0.55
D	Slag + Waterglass + 1% V	0.55
E	Slag + NaOH	0.50

2.2. Carbonation test

Cubic specimens (4-cm) were prepared to Spanish and European standard UNE-EN 197-1. The waterglass-

TABLE IV Physical and chemical properties of admixtures

Admixture	V	SRA
Solid content (%)	25	–
pH	6.80	10.70
Density (g/cm^3)	1.14	1.00
Rotational viscosity (MPa)	24.13	26.93
Intrinsic viscosity (ml/g)	55.98	5.70
% C	34.05	57.27
Na (ppm)	38950	1.4
K (ppm)	160	n.d

n.d.: not identified.

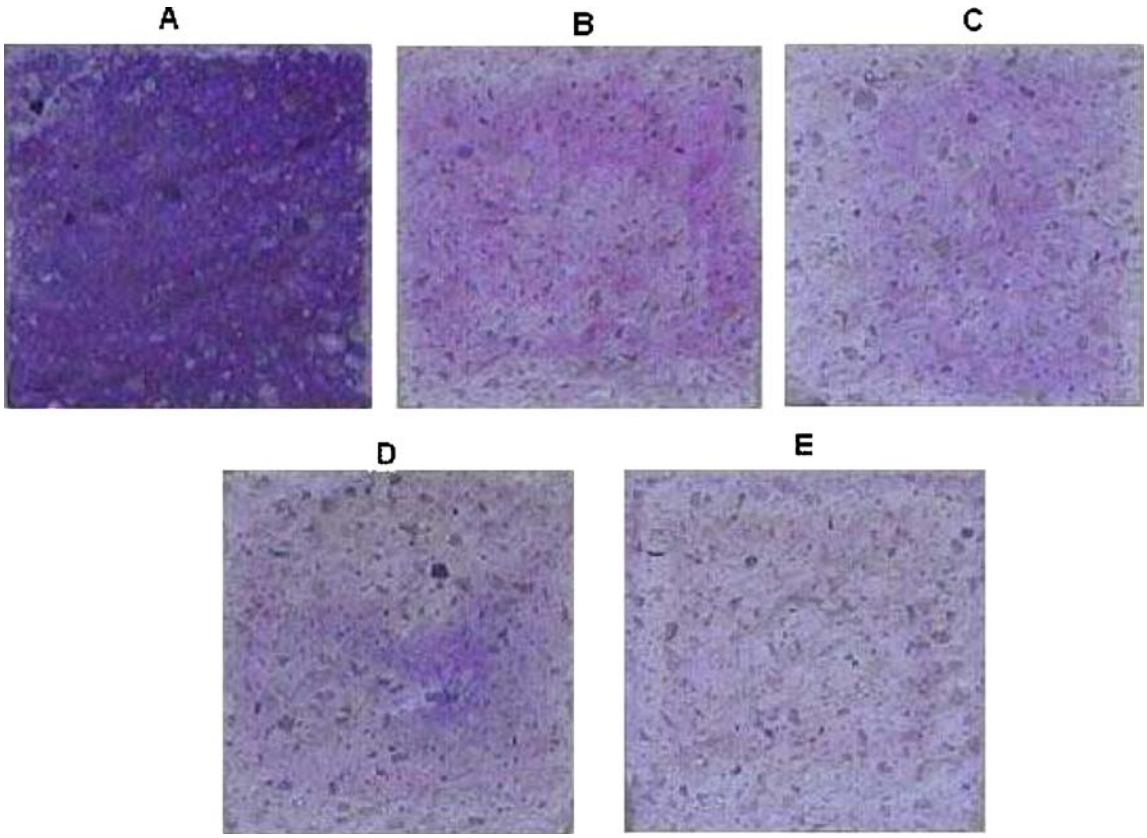

Figure 1 Carbonation front in mortar specimens after four months of exposure (see Table III for mortar identification).

activated slag specimens with and without admixtures were de-moulded after 48 h, while the NaOH-activated slag specimens were de-moulded after 24 h. In all cases, the specimens were kept in a moist closet for 28 days, whereafter they were placed in the carbonation chamber.

This carbonation chamber consisted of a closed cabinet where the relative humidity was kept at 43.2% with a K_2CO_3 solution [28]. Some of the specimens were protected with insulation tape on all but one side. The chamber was CO_2-saturated by filling it with the gas twice a day. The mortar specimens were removed after four and eight months of exposure.

2.3. Tests conducted

The phenolphthalein test was used to measure the carbonation front on the side exposed to CO_2, as described in [29].

Both carbonated and non-carbonated specimens were tested for the following:

(a) Determination of compression strength to European standard EN 196-1.

(b) X-ray diffraction (XRD). A Philips PW-1730 diffractometer was used. Values were recorded at 2θ intervals from 5 to 60°.

(c) Fourier transformer infrared (FTIR) spectrometry. An ATIMATTSON, Genesis FTIR-TM spectrometer was used. KBr pellets (1 mg of sample to 300 mg of KBr) were prepared. Frequencies were scanned across a range of 4000 to 400 cm^{-1}.

(d) Hg intrusion porosimetry (MIP). A Micromeritics 9320 porosimeter was used.

(e) Scanning electron microscopy (SEM/EDX). The equipment used comprised a JOEL 5400 microscope attached to an Oxford-Link ISIS EDX microanalysis unit.

3. Results

3.1. Tests conducted on mortars

3.1.1. Depth of carbonation front

The results of treating the surface of the mortar specimens carbonated for four months with phenolphthalein are shown in Fig. 1. The mortar or concrete surface turns magenta with this indicator when the pH of the aqueous phase is over 9.0, but remains colourless when carbonation lowers the pH to under that value. The data showed that carbonation was slight in Portland cement, with the front no deeper than 1 mm. The alkali-activated slag mortars, on the contrary, showed much deeper and more intense carbonation. When the activator used was a waterglass solution, a carbonation front up to 10 mm deep was observed, and the specimen was partially carbonated at even greater depths. When NaOH was the alkali activator, however, a 1-mm, non-carbonated front was observed on the outer edge of the specimen, followed by a 3-mm deep carbonated front. Specimen interiors were also observed to be partially carbonated.

The addition of the vinyl copolymer and polypropylenglycol derivative admixtures had no effect on the

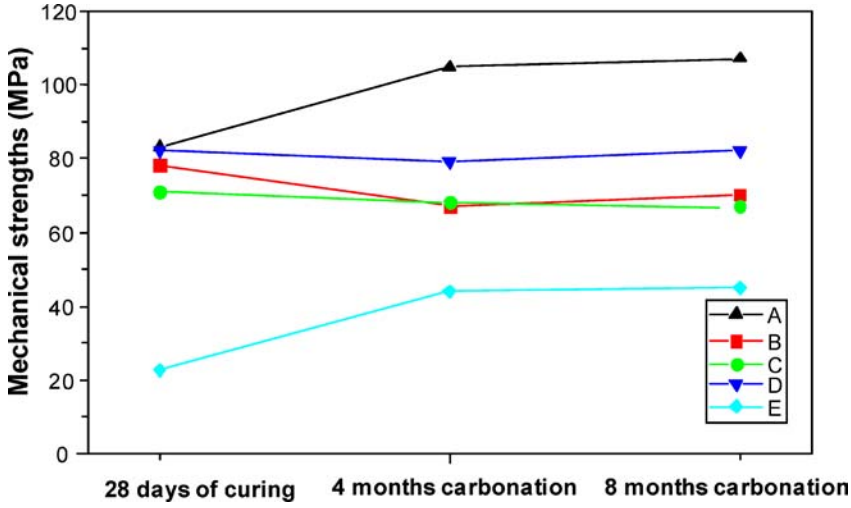

Figure 2 Mechanical strength during carbonation test (see Table III for mortar identification).

results for waterglass-activated slag mortars after carbonation. In both cases, the partial carbonation of specimen interiors was comparable to the results for mortars with no admixtures.

3.1.2. Mortar mechanical strength

Fig. 2 shows mortar strength against carbonation time.

Portland cement mortars showed a 26% increase in mechanical strength after 4 months of carbonation, compared to the 28-day values; however there is no increase in mechanical strength between four and eight months of carbonation.

The effect of carbonation on the strength of AAS mortars depended on the type of alkali activator used. In the absence of any admixtures, the mechanical strength of waterglass-activated slag mortars declined by 14% after four months of carbonation; no further decline was observed after eight months of exposure. The inclusion of admixtures V and SRA had virtually no effect on the mechanical performance of mortar specimens subjected to carbonation, although strength was consistently higher in the mortars with the vinyl admixture.

The mechanical strength behaviour of NaOH-activated slag mortars was similar to Portland cement mortars, although the values were much lower in the former. The slag mortars activated with a NaOH solution showed increases in mechanical strength of up to 93% after four months, with no change in these values between four and eight months of carbonation.

3.1.3. X-ray diffraction (XRD)

Fig. 3 shows the various crystalline phases compounding the slag and cement mortars before and after carbonation process.

The diffractograms for ordinary Portland cement mortars (Fig. 3a) after carbonation indicate that carbonation was not extensive, inasmuch as large amounts of portlandite (2θ = 18.08°, 34.08° and 47.13°) were detected in the sample after eight months of exposure. Calcite (2θ = 29.41°, 39.40° and 43.15°) was observed in the 28-day, pre-carbonation samples and the diffraction lines indicative of this compound grew slightly more intense as carbonation progressed.

The diffractograms for the waterglass-activated slag (Fig. 3b) show that calcium carbonate was present in the form of calcite after a curing specimens for 28 days. After four and eight months of carbonation, vaterite (2θ = 24.86, 27.03° and 32.71°) and traces of aragonite (2θ = 26.23°, 27.23° and 45.85°) as well as natron ($Na_2CO_3 \cdot 10H_2O$) were detected, in addition to calcite. Because of its semi-crystalline nature (2θ = 7.07, 29.09, 31.96 and 49.83), the CSH gel formed was difficult to identify with XRD techniques, although the existence of a low intensity signal of around 2θ = 29.18° might be associated with the presence of such a gel. The inclusion of the organic admixtures (Fig. 3c and d) did not affect the mineralogical composition of the carbonated pastes, which was essentially the same as the mortars with no such admixtures.

Hydrocalcite ($Mg_6Al_2(CO_3(OH)_{16} \cdot 4H_2O$) was detected in the pre-carbonation diffractograms for NaOH-activated slag mortars (Fig. 3e), as well as in the carbonated samples. The phases found after carbonation—calcite, aragonite, vaterite and natron — were the same as in the waterglass-activated slag mortars. In this case, a much smaller proportion of vaterite than of aragonite was formed, which contrasts with the results for carbonated waterglass-activated slag mortars. The diffraction line assigned to the CSH gel—2θ = 7.07°—could be detected at 28 days, although it progressively disappeared as carbonation progressed.

3.1.4. Fourier transform infrared spectroscopy (FTIR)

The infrared spectra for the various mortars are shown in Fig. 4. The Portland cement spectra (Fig. 4a) show that calcite (1429 cm^{-1}, 875 cm^{-1} and 710 cm^{-1}) was

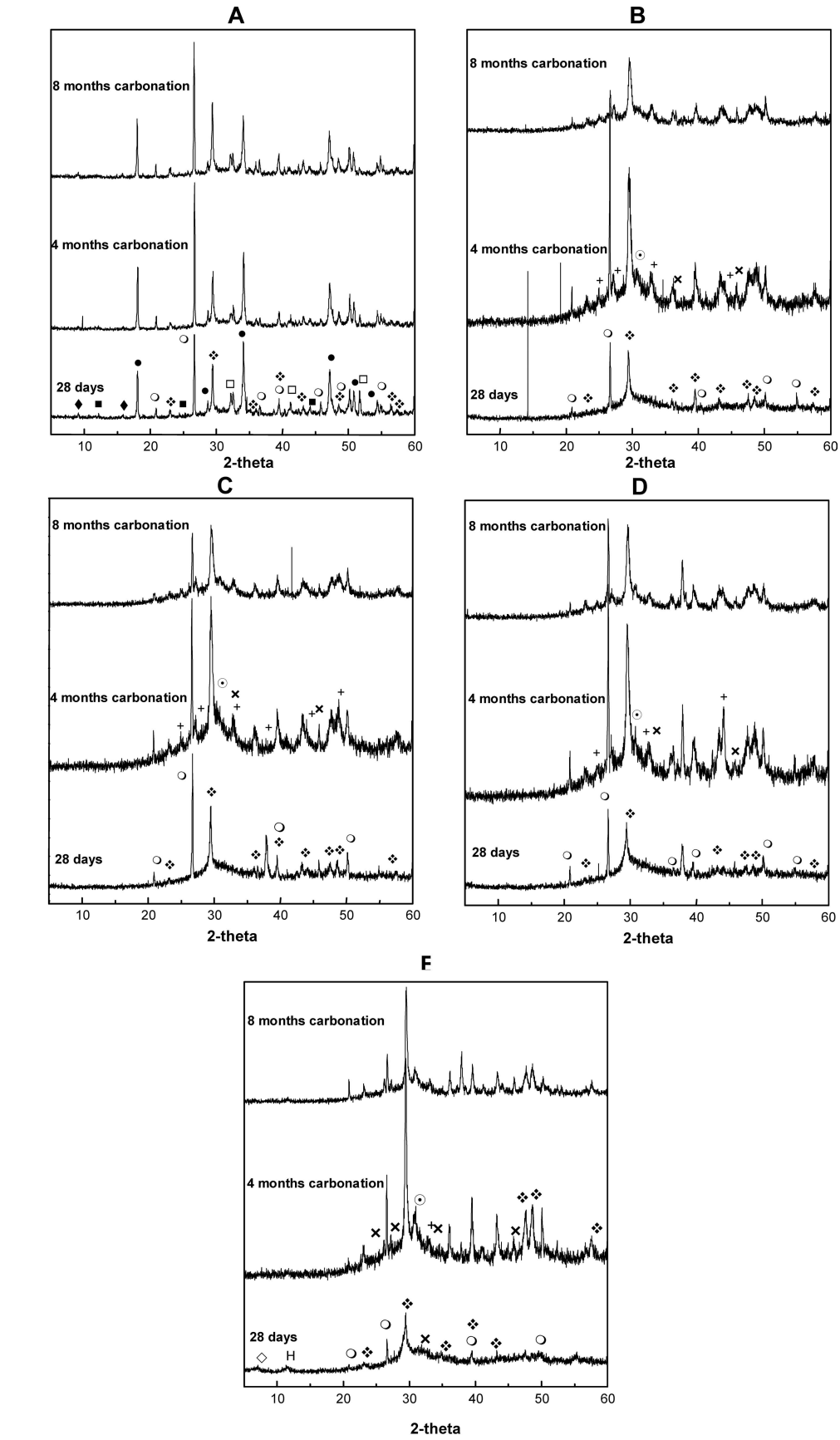

Figure 3 Mortar diffractograms before and after carbonation (see Table III for mortar identification).

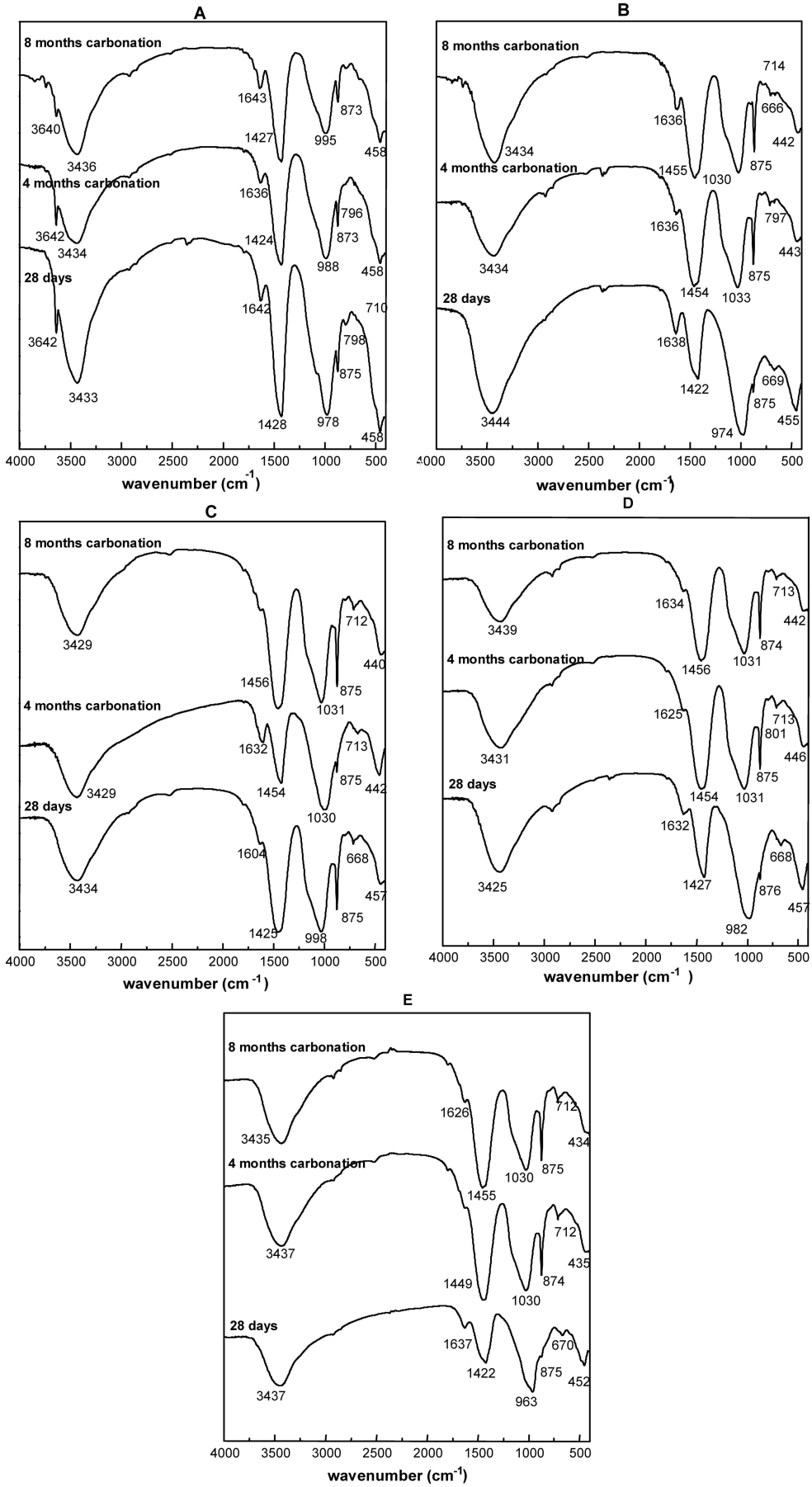

Figure 4 Mortar infrared spectra before and after carbonation (see Table III for mortar identification).

TABLE V Total porosity and average pore diameter

Mortar	Total porosity (%)			Average pore diameter (μm)		
	28 days	4 months carbonation	8 months carbonation	28 days	4 months carbonation	8 months carbonation
A	11.00	11.64	9.91	0.0125	0.0300	0.0267
B	10.25	9.36	10.33	0.0110	0.0270	0.0286
C	12.85	8.65	9.15	0.0419	0.0287	0.0449
D	10.30	10.42	9.83	0.0127	0.0433	0.0400
E	20.24	15.44	15.08	0.0870	0.0671	0.0593

present prior to the carbonation test, as a result of mortar weathering. As carbonation advanced, the vibration band at around 3642 cm^{-1}, corresponding to the O–H bond in portlandite, was observed to weaken. The Si–O vibration band, in turn, shifted slightly, from 978 to 995 cm^{-1}, indicating the formation of a CSH gel with a smaller Ca content.

The waterglass-activated slag spectra (Fig. 4b) show that calcite was present in the 28-day specimens due to surface carbonation. After four and eight months of exposure to carbonation, a very wide band, centred on 1454 cm^{-1}, was detected. This band is attributed to poorly crystallized vaterite (at 1450 cm^{-1}, 875 cm^{-1} and 710 cm^{-1}) and aragonite (1483 cm^{-1}, 1452 cm^{-1}, 875 cm^{-1} and 713 cm^{-1}), together with the initial calcite. The presence of natron could not be confirmed (at around 1460 cm^{-1}, 1418 cm^{-1}, 875 cm^{-1}, 860 cm^{-1} and 712 cm^{-1}), because its vibration bands and the calcite, vaterite and aragonite bands overlap. The Si–O vibration band shifted from 974 to 1033 cm^{-1} as a result of carbonation and the important decalcification of the CSH gel. This shift was much broader than in the Portland cement. Aragonite, together with the initial calcite and possibly natron, were also observed to form in the waterglass-activated samples that contained admixtures (Fig. 4c and d). The inclusion of both the vinyl copolymer and the polypropylenglycol derivative was observed to increase the Si–O vibration band wave number on the pre-carbonation spectra to 998 and 982 cm^{-1}, respectively, up from the values for the admixture-free samples. Nonetheless, after carbonation, this band shifted to 1030 cm^{-1}, the same value as recorded for activated slag mortars with no admixture.

Finally, the post-carbonation spectra for the NaOH-activated slag (Fig. 4e) showed that aragonite, vaterite and possibly natron were present, in addition to the initial calcite. Here also, carbonation of the CSH gel caused the Si–O vibration band to shift to higher wave numbers, from 963 to 1030 cm^{-1}, owing to the lower Ca content in the gel.

3.1.5. Mercury intrusion porosimetry

The pore size distribution, total porosity and average pore diameter of the different mortars are given in Tables V and VI.

The total porosity and average pore diameter declined in Portland cement mortars as a result of 4 months carbonation. After eight months of exposure, however, the pore diameter was found to increase. As far as pore size distribution is concerned, the percentage of pores ranging in size from 10 to 0.1 μm fell, while the proportion of pores with diameters ranging from 0.1 to 0.01 μm fell substantially.

Waterglass-activated slag mortars showed a slight decline in total porosity as carbonation progressed, while

TABLE VI Pore size distribution

Mortar		Percentage (%)						
		Pore diameter (μm)						
		>200	200–100	100–10	10–1.0	1.0–0.1	0.1–0.01	<0.01
A	28 days	1.50	1.00	1.67	2.50	12.69	76.79	3.84
	4 months carbonation	2.33	1.29	3.11	3.11	10.10	69.17	10.88
	8 months carbonation	2.15	1.20	2.63	7.65	20.33	55.74	10.29
B	28 days	2.22	1.11	3.88	18.30	8.32	29.50	36.60
	4 months carbonation	1.27	1.09	3.27	11.82	19.45	41.27	21.82
	8 months carbonation	1.09	1.53	3.06	15.72	15.50	38.43	24.67
C	28 days	2.23	1.01	3.04	15.21	7.71	28.80	41.99
	4 months carbonation	1.41	1.18	3.07	10.85	19.92	42.22	23.35
	8 months carbonation	1.04	1.46	3.33	4.58	25.62	42.29	21.67
D	28 days	1.60	0.80	2.59	23.55	8.78	26.35	36.33
	4 months carbonation	1.45	1.45	8.07	9.32	21.74	37.47	20.50
	8 months carbonation	1.12	1.56	2.45	10.49	25.22	38.17	20.98
E	28 days	1.31	0.71	2.83	12.33	31.04	48.73	3.03
	4 months carbonation	0.69	0.55	2.08	4.71	35.59	46.81	9.56
	8 months carbonation	0.85	1.56	1.98	2.12	35.41	49.15	8.92

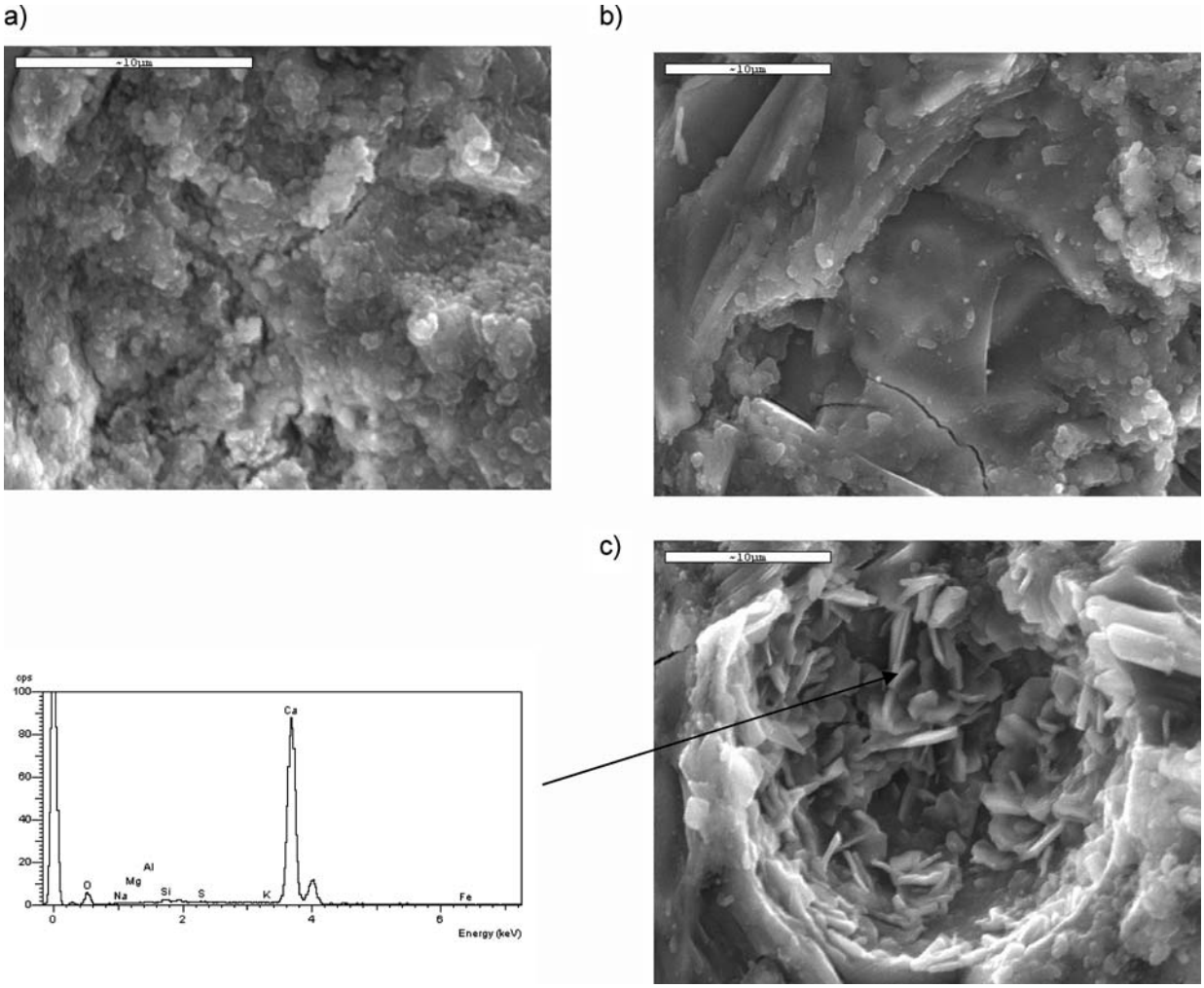

Figure 5 Portland cement mortars; (a) before carbonation, (b) after 8 months of exposure to a CO_2-saturated environment, (c) calcite after 8 months of carbonation.

the average pore size increased significantly as a result of the increase in the percentage of pores with a size of from 1.0 to 0.01 μm and a drop in the number of pores with diameters of under 0.01 μm. The inclusion of organic admixtures, in turn, induced a steep decrease in the percentage of pores ranging in size from 10 to 1.0 μm.

The largest drop in total porosity and average pore size conduct to the refinement of the structure of the paste was observed in NaOH solution-activated slag mortars. The figures given in Table VI show that as carbonation advanced, the percentage of pores ranging in size from 10 to 0.1 μm fell, while the percentage of pores with diameters of under 0.01 μm grew during the first 4 months of carbonation.

3.1.6. Scanning electron microscopy

Microstructural studies were conducted on the various mortars after they had been cured for 28 days and after eight months of exposure to carbonation. The micrographs in Figs 5–9 show significant differences in the effect of carbonation on the different mortars.

Carbonation was observed to increase compaction and density in Portland cement mortars (Fig. 5). Furthermore, the pores of the matrix contained a crystal precipitate—calcium carbonate—composed nearly exclusively of Ca.

Differences were likewise observed in the effect of carbonation on AAS mortars depending on the activator solution used.

When the activator was waterglass, the pastes became substantially less cohesive and more granular than at the age of 28 days (Fig. 6b). At the same time, whitish, spongy particles with a very low Ca content were observed in these mortars, whose chemical composition consisted primarily of Si, Al, Na and Mg. The inclusion of organic admixtures to waterglass-activated slag mortars (Figs 7 and 8) did not affect mortar performance after carbonation.

When a NaOH solution was used as the alkali activator, carbonation increased matrix density (Fig. 9) as it did in Portland cement mortars. Nonetheless, white particles with a low Ca content, similar to the ones analyzed in waterglass-activated slag mortars, were also found in the NaOH pastes, which likewise contained a high Ca-content crystal precipitate in the pores.

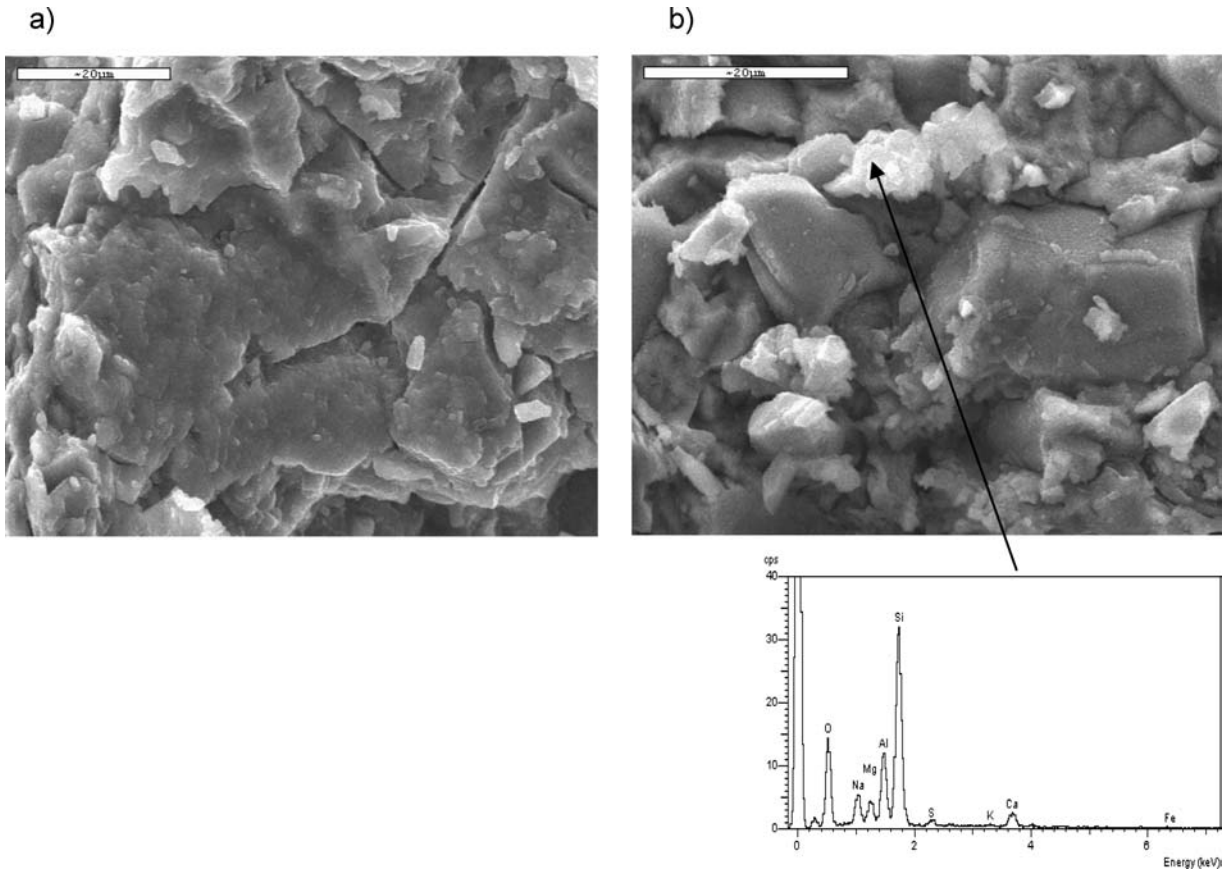

Figure 6 Waterglass-activated slag mortars; (a) before carbonation, (b) after 8 months of exposure to a CO_2-saturated environment.

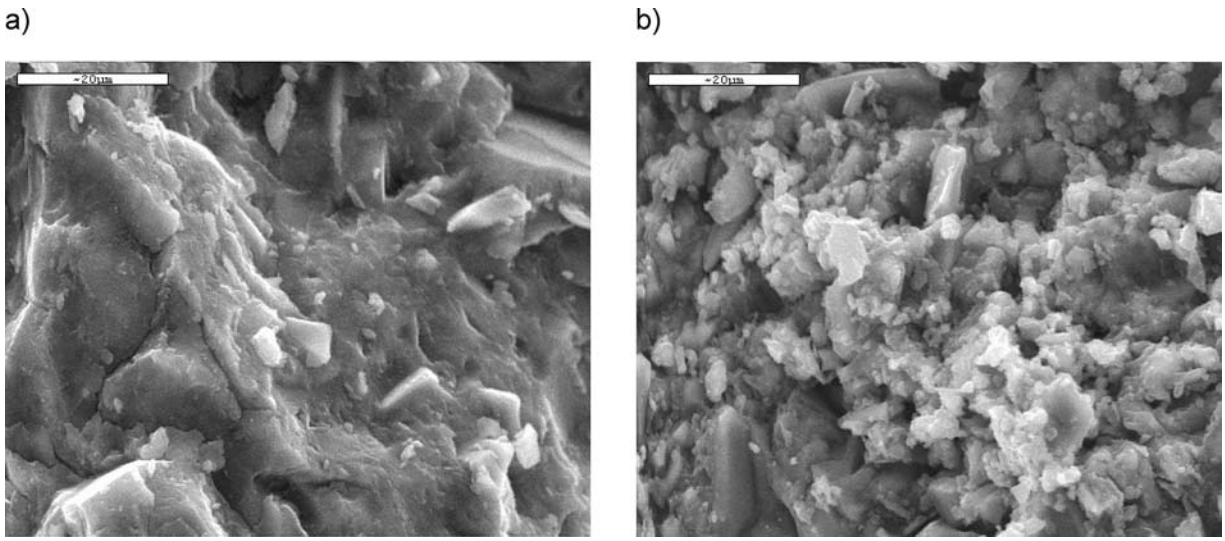

Figure 7 Waterglass-activated slag mortars with a vinyl copolymer admixture; (a) before carbonation, (b) after 8 months of exposure to a CO_2-saturated environment.

4. Discussion

The carbonation front test showed that carbonation is deeper and more intense in alkali-activated slag mortars than in the respective Portland cement mortars. These results concur with other authors' findings [25, 26]. The present study also found, however, that the behaviour of AAS mortars after carbonation depends on the type of activator used. Further to these results, when waterglass was the activator, mechanical strength declined slightly after carbonation (by around 14%), whereas when the activator was a NaOH solution, strength increased (by over 90%), just as it did in Portland cement mortars.

Carbonation has been more or less thoroughly described in Portland cement mortars and concretes [21, 29]. The most soluble species in the cement paste is

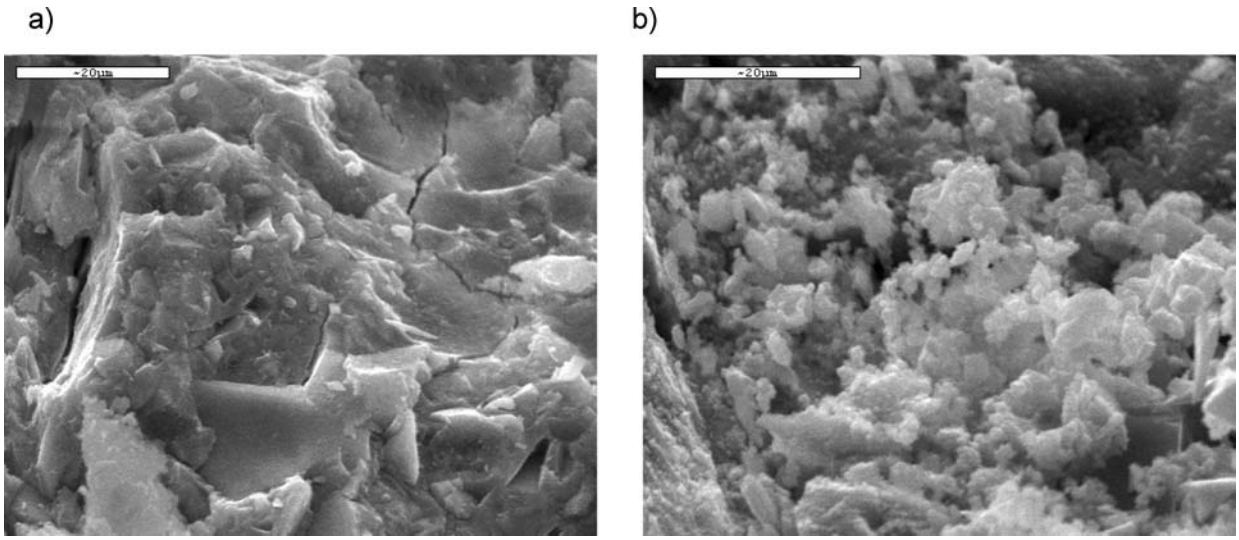

Figure 8 Waterglass-activated slag mortars with a polypropylenglycol derivative admixture; (a) before carbonation. (b) after 8 months of exposure to a CO_2-saturated environment.

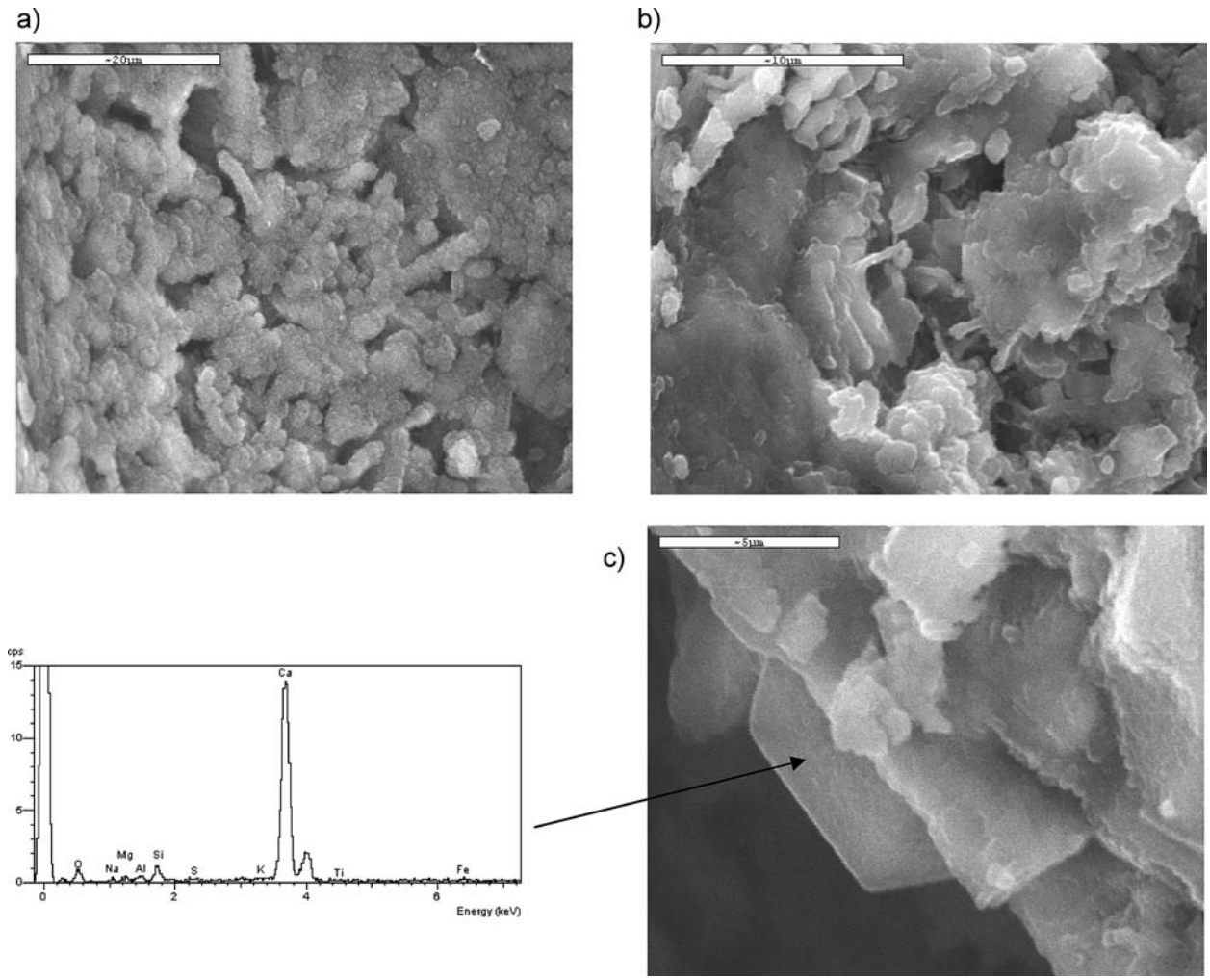

Figure 9 NaOH-activated slag mortars; (a) before carbonation, (b) after 8 months of exposure to a CO_2-saturated environment, (c) calcite after 8 months of carbonation.

portlandite or $Ca(OH)_2$. Initially CO_2 acts on this compound, yielding $CaCO_3$, primarily in the form of calcite, according to the XRD findings (Fig. 3a). In very deep or highly accelerated carbonation systems, CO_2 may also interact with the CSH gel in the paste, leading to its decalcification and increasing the length of silicate chains. Evidence for this development is provided by FTIR (Fig. 4a), in the shift observed in the Si=O vibration band associated with the CSH gel from 978 cm^{-1} to higher frequencies (~990–995 cm^{-1}).

The results obtained showed that carbonation is shallow in Portland cement mortars (barely 1 mm thick). The precipitation of $CaCO_3$ in the matrix as a result of carbonation (Fig. 5) covered the pores and prevented more CO_2 to penetrate any deeper into the mortar. This, in conjunction with ongoing hydration, yielded a denser and more compact mortar (with a decline in average pore size), all of which explained the increase in the mechanical strength observed.

In AAS mortars, the results showed that carbonation takes place directly on the CSH gel, as Bakharev [26] concluded. This was observed in the FTIR (Fig. 4b–e) results, and more specifically in the shift in the Si=O band attributable to the CSH gel from 963–998 cm^{-1} to frequency values of 1030 cm^{-1}, a development indicative of the formation of a silicate with a very low calcium content.

This finding was observed in both waterglass and NaOH-activated slag mortars, although its impact differed greatly in the two cases.

Deja [25] concluded that the low total porosity and average pore size in waterglass-activated slag concretes increased their resistance to carbonation. In the present study, however, CO_2 penetration was found to be enhanced, despite the low porosity. This may be interpreted as follows: waterglass-activated mortars and concretes shrink considerably during the drying process [30], leading to the formation of a large number of microscopic cracks (Fig. 6) that facilitate the entry of CO_2 inside the mortar. The interaction between the CO_2 and the CSH gel formed in these pastes generates decalcification in the latter and the appearance of spongy white particles with a low Ca content whose composition is primarily Si, Al, Mg and Na (Fig. 5). Decalcification prompts a loss of cohesion in the mortar (confirmed by SEM) and induces larger pore sizes. This would explain the decline in chemical strength, which does not appear to be mitigated by admixtures.

Carbonation also conducted decalcification of the CSH gel in NaOH-activated slag mortars, but in this case, as in Portland cement mortars, the result was greater internal cohesion with a decline in porosity and greater mechanical strength. This differential behaviour can be attributed to the differences in the composition and structure of the CSH gel formed when one or the other type of activator was used.

It is generally agreed [30, 31] that the nature of the alkali activator determines the composition and structure of the main reaction product in these pastes, a CSH gel. When waterglass is the activator [20, 31], the CSH gel formed is characterized by long silicate chains (with around eight links), a low Ca/Si ratio of around 0.8 and high Al content in tetrahaedral positions in the controversial tetrahedra. When NaOH is the activator, the gel has shorter chains (with 5–8 inks), higher Ca/Si ratios—of around 1.2—and Al in its structure. It may be deduced that the CSH formed in NaOH-activated slag pastes is more like the CSH gel in Portland cement pastes. The higher Ca content of the CSH gel in NaOH-activated slag mortars may generate greater amounts of $CaCO_3$ during carbonation, and this product might precipitate into and cover the pores of the mortar. This effect, observed under SEM (Fig. 9) studies for both these and Portland cement mortars, may contribute to the enhanced cohesion observed.

Further study is nonetheless required to explain these differences in behaviour as a whole.

5. Conclusions

1. Carbonation is deeper and more intense in alkali-activated slag than in Portland cement mortars.

2. Regardless of the type of activator used, carbonation in activated slag mortars takes place on and decalcifies the CSH gel.

3. Mortar properties after carbonation differ depending on the nature of the alkali activator used.

   3.1. When waterglass is the alkali activator, the decalcification of the CSH gel prompted by carbonation leads to a loss of cohesion in the matrix and an increase in porosity and decline in mechanical strength.

   3.2. When NaOH is the alkali activator, carbonation enhances mortar cohesion, possibly as a result of the precipitation of greater amounts of calcium carbonate in the pores, causing a decline in total porosity and average pore size and consequently an increase in mechanical strength.

4. The inclusion of vinyl copolymer and polypropylenglycol derivative admixtures in waterglass-activated slag systems has no impact either on mortar behaviour after carbonation or on the nature of the reaction products formed.

Acknowledgements

Funding for project MAT 2001-1490 was provided by the Spanish Ministry of Science and Technology (MCyT). The authors wish to thank Dr M. Teresa Blanco for her selfless assistance and valuable suggestions for this research, and A. Gil, L. Ureña, J. L. García and M. M. Alonso for their support in the tests conducted for this study.

References

1. V. D. GLUKHOVSKY, G. S. ROSTOVSKAJA and G. V. YRUMYNA, in 7th International Congress Chemistry Cement (Paris) (1980) vol. 164–168, p. 3.

2. P. V. KRIVENKO, in 9th International Congress Chemistry Cement (New Delhi) (1992) vol. 4, p. 481.
3. S. D. WANG, K. L. SCRIVENER and P. L. PRATT, *Cement and Concrete Res.* **24**(6) (1994) 1033.
4. A. FERNÁNDEZ-JIMÉNEZ, F. PUERTAS and J. G. PALOMO, *ibid.* **29**(3) (1999) 593.
5. S. D. WANG, X. C. PU, K. L. SCRIVENER and P. L. PRATT, *Advances in Cement Res.* **7**(27) (1995) 93.
6. F. PUERTAS, *Mater. Construcc.* **45**(239) 53.
7. T. BAKHAREV, J. SANJAYAN and Y.-B. CHENG, *Cement and Concrete Res.* **29** (1999) 113.
8. C. SHI, *ibid.* **26** (1996) 1789.
9. T. BAKHAREV, J. G. SANJAYAN and Y.-B. CHENG, *ibid.* **32** (2002) 211.
10. F. PUERTAS, R. DE GUTIERREZ, A. FERNÁNDEZ-JIMÉNEZ, S. DELVASTO and J. MALDONADO, *Mater. Construcc.* **52**(267) (2002) 55.
11. C. SHI, *Advances in Cement Res.* **15**(2) (2003) 77.
12. PU XINCHENG, YANG CHANGHUI and LIU FAN, Second International Conference Alkaline Cements and Concretes (1999) p. 717.
13. T. BAKHAREV, J. G. SANJAYAN, and Y.-B. CHENG, *Cem. and Con. Res.* **33** (2003) 1607.
14. F. PUERTAS, T. AMAT, A. FERNÁNDEZ-JIMÉNEZ, T. VÁZQUEZ, *ibid.* **33** (2003) 2031.
15. XU BIN and PU XINCHENG, Second International Conference Alkaline Cements and Concretes (1999) p. 101.
16. B. TAILING and J. BRANDSTETR, in Proc. 3rd Int. Conf. On Fly Ash, Silica Fume, Slag and Natural Pozzolans in Concrete, Trondheim, (1989), 2, SP114-74, p. 1519.
17. R. MEJÍA DE GUTIERREZ, J. MALDONADO, C. GUTIÉRREZ, *Mater. Construcc.* **54**(276) (2004) p. 87.
18. S. D. WANG. and K. SCRIVENER, *Cem. Con. Res.* **25**(3) (1995) p. 561.
19. J. I. ESCALANTE-GARCÍA, A. F. FUENTES, A. GOROKOVSKY, P. E. FRAIRE-LUNA and G. MENDOZA-SUAREZ, *J. Am. Ceram. Soc.* **86**(12) (2003) 48.
20. A. FERNÁNDEZ-JIMÉNEZ, F. PUERTAS, I. SOBRADOS and J. SANZ, *ibid.* **86**(8) (2003) 1389.
21. N. R. SHORT, A. R. BROUGH, A. M. G. SENEVIRATNE, P. PURNELL and C. L. PAGE, *J. Mater. Sci.* **39** (2004) 5683.
22. Y. F. HOUST and F. H. WITTMANN, *Cem. Concr. Res.* **32** (2002) 1923.
23. K. BYFORS, *et al.* in Proc. 3rd Int. Conf. on Fly Ash, Silica Fume, Slag and Natural Pozzolans in Concrete. Trondheim (1989) SP114-70, vol. 2, p. 1547.
24. X. C. PU, *et al.* "Sumary reports of Research on Alkali-Activated Slag Cement and Concrete" (Chongqing Institute of Architecture and Engineering, 1988), 6 vols (in Chinese).
25. J. DEJA, *Sil. Ind.* **67**(3–4) (2002) 37.
26. T. BAKAREV J. G. SANJAYAN and Y.-B. CHENG, *Cem. Concr. Res.* **31** (2001) 1277.
27. E 104-02 ASTM, "Maintaining Constant Relative Humidity by Means of Aqueous Solutions".
28. UNE 112-011-94. Corrosión en armaduras. "Determinación de la profundidad de carbonatación en hormigones endurecidos y puestos en servicio.
29. A. M. NEVILLE, "Properties of Concrete" Edited by Addison Wesley Longman, 4th edition (1995).
30. C. SHI, *et al.* in Proc. 9th Int. Congr. On the Chemistry of Cement (New Delhi, 1992), vol. 3, p. 298.
31. F. PUERTAS, A. FERNÁNDEZ-JIMÉNEZ, M. T. BLANCO-VARELA, *Cem. Con. Res.* **34** (2004) 139.

Received 19 January
and accepted 2 May 2005